Transactions, SMiRT-24
BEXCO, Busan, Korea - August 20-25, 2017
Division III

MISSILE IMPACT ON REINFORCED CONCRETE BARRIER SLAB USING VARIOUS FAILURE MODELS

Mrigendra Nath Ray[1], Shivam Srivastava[2], Nishikant R. Vaidya[3], and Eddie Guerra[3]

[1] Consultant (Nuclear Power) India
[2] Larsen Toubro, Baroda, India
[3] RIZZO Associates, Pittsburgh, USA

ABSTRACT

This paper examines the effects of impact of a steel, semi-rigid missile on concrete barrier. The concrete barrier resembles the protective cover on important safety systems in a nuclear plant, and the missile considered here represents missiles potentially ejected due to structural failure associated with various rotating machinery and high-pressure components installed in the plant operating area. Although these types of missiles eject in random directions, the study reported here assumes for simplicity that the missiles impact the barrier perpendicular to the plane of the barrier. The barrier is assumed to be made of reinforced concrete, a commonly used material for this purpose due to its structural stiffness and ductility for absorbing impact energy. Two failure models are evaluated – 1) Brittle Cracking model and 2) Concrete Damaged Plasticity model. Based on the analysis results such as material stresses/displacements and predictions of local damage in the impact zone, the study evaluates critical barrier thickness to prevent loss of barrier function and assesses empirical methods relative to the finite element results.

INTRODUCTION

The study reported here evaluates missile impact on concrete barrier used to protect nuclear power plant safety systems and components. In this study, internally generated missiles inside and outside containment are represented by a cylindrical object made of carbon steel impacting the target at a very high velocity. This study examines the material behavior of plain and reinforced concrete barriers. The responses of the barriers are analyzed using the computer program ABAQUS (version 6.12). The analysis is performed in the explicit domain for two different failure models of concrete: the Brittle Cracking (BC) model and the Concrete Damaged Plasticity (CDP) model.

Physics Of Stress-Strain Behavior Of Reinforced Concrete

The two primary failure mechanisms in concrete are crushing due to compression and cracking under tension. This paper considers only the uniaxial state of stress in concrete because this closely matches the stress state resulting from missile impact.

Stress-Strain Relationships Used In The Analysis

Ideally, the constitutive relationships for concrete and rebar steel would be based on test data. For purposes of this paper, these relationships are based on published literature (Hsu and Hsu, 1994; Mokhatar and Abdullah, 2012).

Figure 1 presents the stress-strain relationship for uniaxial compression in concrete as developed by Hsu and Hsu in 1994 based on numerous laboratory tests and verified with numerical results. The compressive stress-strain diagram in Figure 1 has two zones – an elastic zone, which is assumed to be in the range of $0\sigma_{cu}$ to $0.5\sigma_{cu}$ in the ascending curve, and an inelastic zone, from $0.5\sigma_{cu}$ in the ascending

curve to 0.3σcu in the descending curve, where σ_{cu} is the characteristic strength (maximum cube strength) of concrete in a compression test.

The stress-strain relationship in the inelastic zone is defined by the compressive stress σ_c and corresponding inelastic strain ε_{in}. The inelastic strain ε_{in} is obtained by deducting the elastic strain ε_{el} from the total strain ε_c shown in Figure 1. Additionally, the damage parameter d_c is defined as the ratio of inelastic strain to total strain. The total strain is obtained from the stress-strain relationship in Figure 1, and the elastic strain is calculated as the ratio of the compressive stress σ_c to the initial tangent modulus of concrete, E_o.

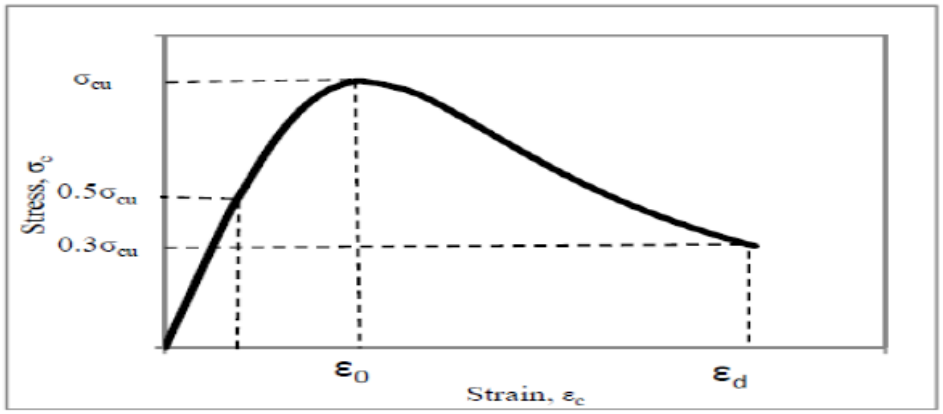

Figure 1. Compressive stress-strain relationship for concrete.

Similarly, Figure 2 shows the tensile stress-strain relationship of concrete (Mokhatar and Abdullah, 2012), in which f_{ct} is the tensile strength based on test data, and ε_t is the corresponding strain. Similar to the behavior in compression, the damage state in tension is defined by the tensile cracking strain ε_{ck}. The cracking strain ε_{ck} is calculated as the difference between total tensile strain ε_t minus the elastic tensile strain ε_{et} for the undamaged concrete. The tensile damage parameter is defined as the ratio of cracking strain to the total tensile strain.

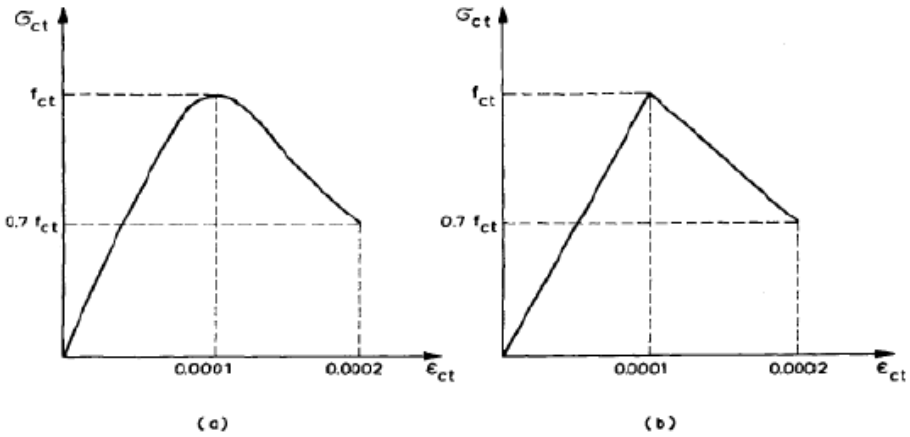

Figure 2. Tensile stress-strain diagram for concrete.

In all cases of the parametric analyses reported here, Grade M50 is used for plain and reinforced concrete, per Indian Standard 456-2000 (Bureau of Indian Standards, 2007). The stress-strain relationship for reinforcing steel is approximated by the relationship for ASTM International (ASTM) Grade A36.

Failure Modes

It is generally accepted that concrete exhibits two primary modes of behavior:

- A brittle mode, in which microcracking gradually transforms into macrocracking, with highly localized deformation.
- A ductile mode, in which microcracks develop uniformly through the specimen, leading to non-localized deformations. This model allows removal of material based on brittle failure criteria.

BC Model For Concrete

The BC model is considered for applications in which the behavior of concrete is dominated by tensile cracking. It is most accurate in applications where brittle behavior dominates such that the assumption that the material is linear elastic in compression is adequate.

CDP Model

The CDP model is primarily intended to provide general capability for the analysis of concrete structures under cyclic and/or dynamic loading. The model is also suitable for the analysis of other quasi-brittle materials, such as rock, mortar, and ceramics, but it is the behavior of concrete that is used in this model to motivate different aspects of the constitutive theory. Under low confining pressures, concrete behaves in a brittle manner; the primary failure mechanisms are crushing in compression and cracking in tension. The brittle behavior of concrete disappears when the confining pressure is sufficiently large to prevent crack propagation. In these circumstances, failure is driven by the consolidation and collapse of the concrete porous microstructure, leading to a macroscopic response that resembles that of a ductile material with work hardening.

Modeling the behavior of concrete under large hydrostatic pressures is out of the scope of the plastic-damage model considered here. The constitutive theory in this section strives to capture the effects of irreversible damage associated with the failure mechanisms that occur in concrete and other quasi-brittle materials under fairly low confining pressures (less than four or five times the ultimate compressive stress in uniaxial compression loading). These effects manifest themselves in the following macroscopic properties:

- Different yield strengths in tension and compression; the initial yield stress in compression is a factor of 10 or higher than the initial yield stress in tension
- Softening behavior in tension as opposed to initial hardening followed by softening in compression
- Different degradation of the elastic stiffness in tension and compression
- Stiffness recovery effects during cyclic loading

PROBLEM DESCRIPTION

Case 1: BC Model

Case 1(a): Plain Concrete Plate Impacted By A Steel Cylinder-Shaped Missile

This case represents the barrier by a 5-meter (m) x 5-m x 20-centimeter (cm) -thick square plate fixed on all four sides. The plate is constructed of Grade M50 plain concrete with a characteristic compressive strength of 50 megapascals (MPa). The impacting missile is represented by a 0.4-m-diameter and 0.5-m-long carbon steel solid cylinder. The steel cylinder is made of carbon steel with a modulus of elasticity of 206 gigapascals and Poisson's ratio of 0.3. Both concrete and steel are modeled in ABAQUS in the explicit domain.

The ABAQUS finite element model represents the concrete plate and the steel cylinder missile by 400 Linear Hex elements (C3D8R) and 135 Linear Hex elements (C3D8R), respectively. The plate is impacted by the steel cylinder at an impact velocity of 150 meters per second (m/sec). The total duration of the impact input and the integration time step used in the analysis are 0.2 seconds (sec) and 0.02 sec, respectively. Missile penetration is observed at the end of the first time step. It exhibits a punching failure in shear as evidenced by the fact that predicted von Mises stresses in the concrete elements away from the boundary of the impact zone are within the allowable tensile stress of Grade M50 concrete, which is $0.7\sqrt{f_{ck}}$, where f_{ck} is the characteristic concrete compressive strength. Figure 3 shows the von Mises stress contour resulting from Case 1(a).

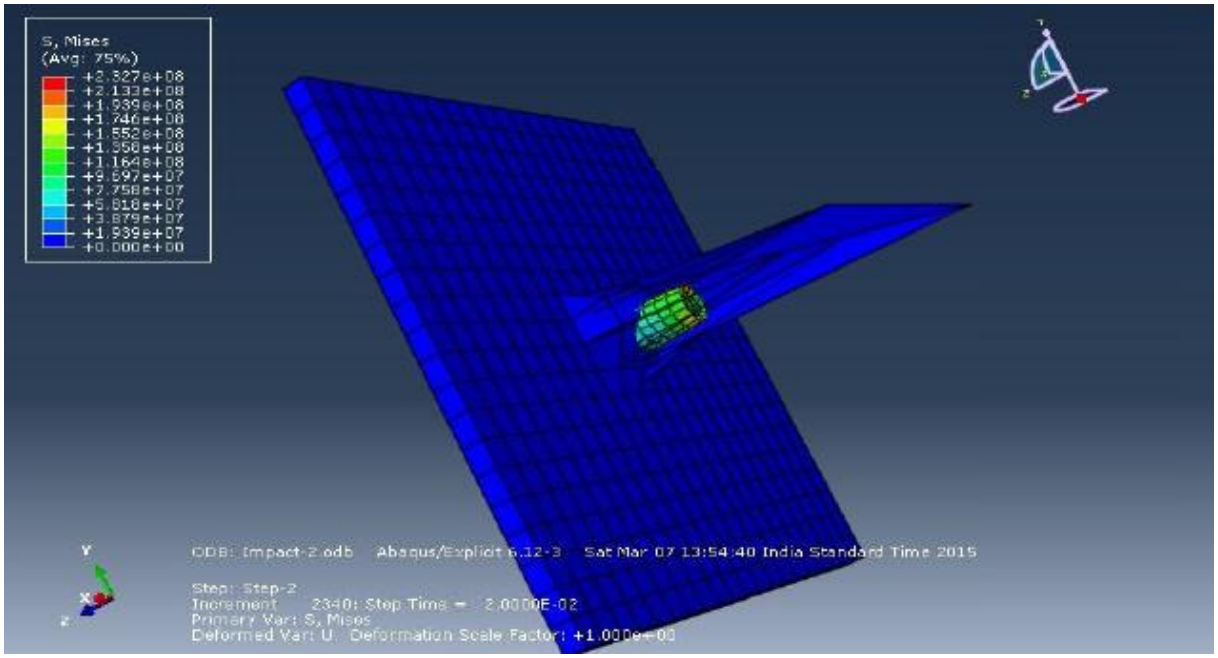

Figure 3. BC model Case 1(a) – von Mises stress results.

Case 1(b): Reinforced Concrete Plate Impacted By A Steel Cylinder-Shaped Missile

This case represents the barrier by a 5-m-square plate, as before; however, the thickness of the plate is increased to 30 cm. The concrete barrier is reinforced with 20-millimeter (mm) rebar spaced at 40 mm, center to center, and placed at mid-thickness. All other parameters, such as boundary conditions, material

properties, and missile configuration and velocity, are the same as in Case 1(a). To account for the effects of the rebar, a more refined mesh is utilized for the barrier as well as for the missile. The concrete barrier, the rebar, and the steel missile are represented by 59225, 18250, and 47300 elements, respectively. The interfaces between the concrete and the rebar, and the concrete and the missile, are modeled using surface-to-surface contact elements. The total duration of impact was 5 milliseconds (ms). Figure 4 and Figure 5 show the von Mises stress contours resulting from Case 1(b).

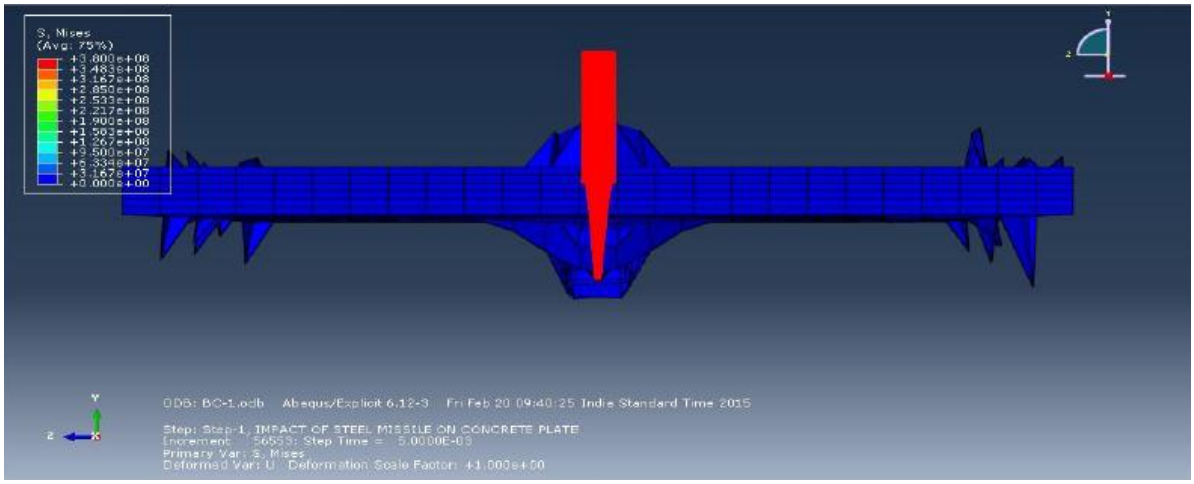

Figure 4. BC model Case 1(b) – von Mises stress results for the concrete and the missile.

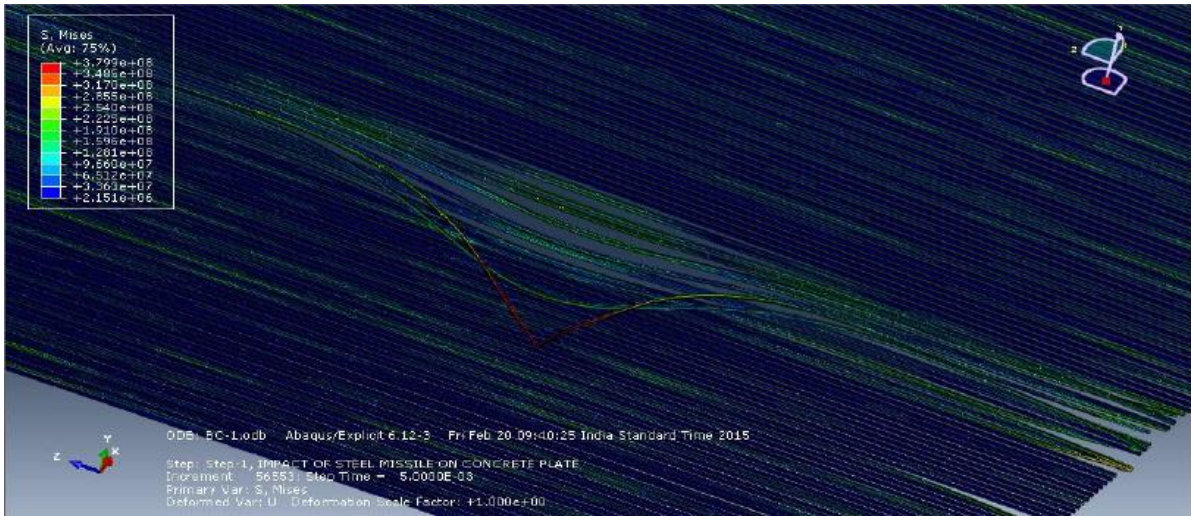

Figure 5. BC model Case 1(b) – von Mises stress results for rebars.

Case 2: CDP Model

Case 2(a): Plain Concrete Plate Impacted By Steel Cylinder-Shaped Missile

The geometry of the plain concrete plate and the missile used in Case 1(a) are not changed for this case, except the total number of elements is increased to 867 and 170 for the concrete and the steel missile, respectively. Figure 6 shows the von Mises stress contour resulting from Case 2(a).

Case 2(b): Reinforced Concrete Plate Impacted By Steel Cylinder-Shaped Missile

The plate geometry and the steel missile are the same as in Case 1(b) to enable observation of any changes in results with respect to the total deformations and stresses in both rebar and concrete elements and comparison with the similar response of the reinforced concrete barrier, assuming the BC model in Case 1(b). Material data for concrete and steel remained the same – Grade M50 for concrete and ASTM Grade A36 for steel for both rebar and the missile. Additionally, the total number of elements considered in this model is the same as in Case 1(b).

Figure 7 and Figure 8 show von Mises stress contours resulting from the analysis of the reinforced concrete plate using the CDP model.

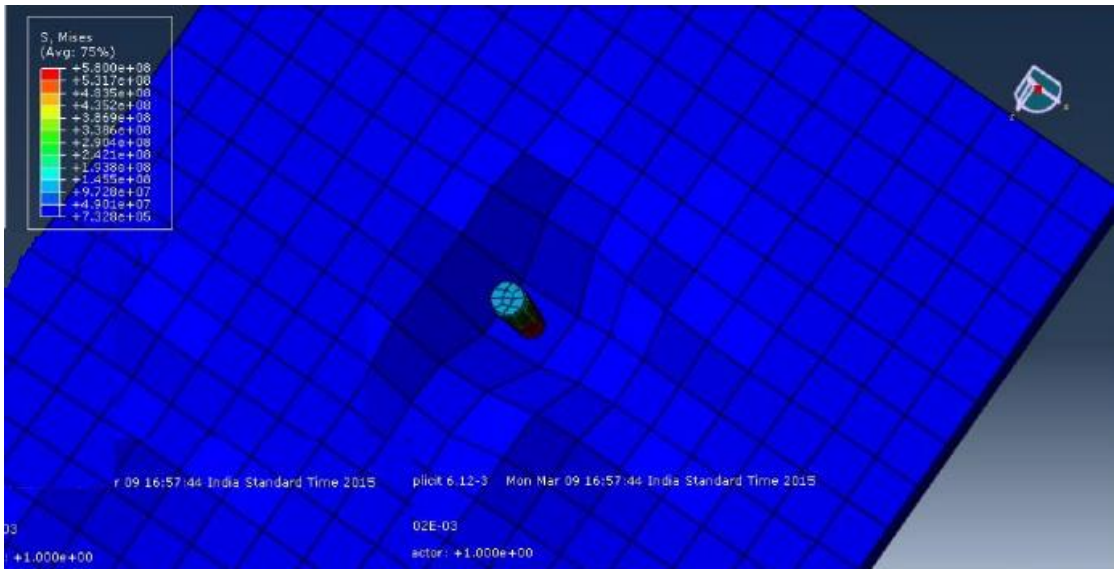

Figure 6. CDP model Case 2(a) – von Mises stress results.

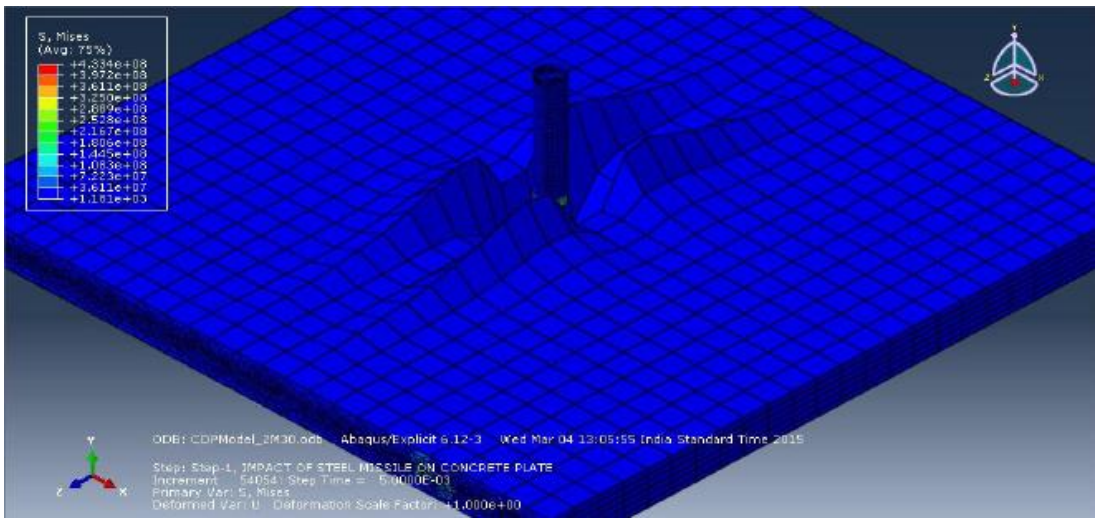

Figure 7. CDP model Case 2(b) – von Mises stress results for the concrete and the missile.

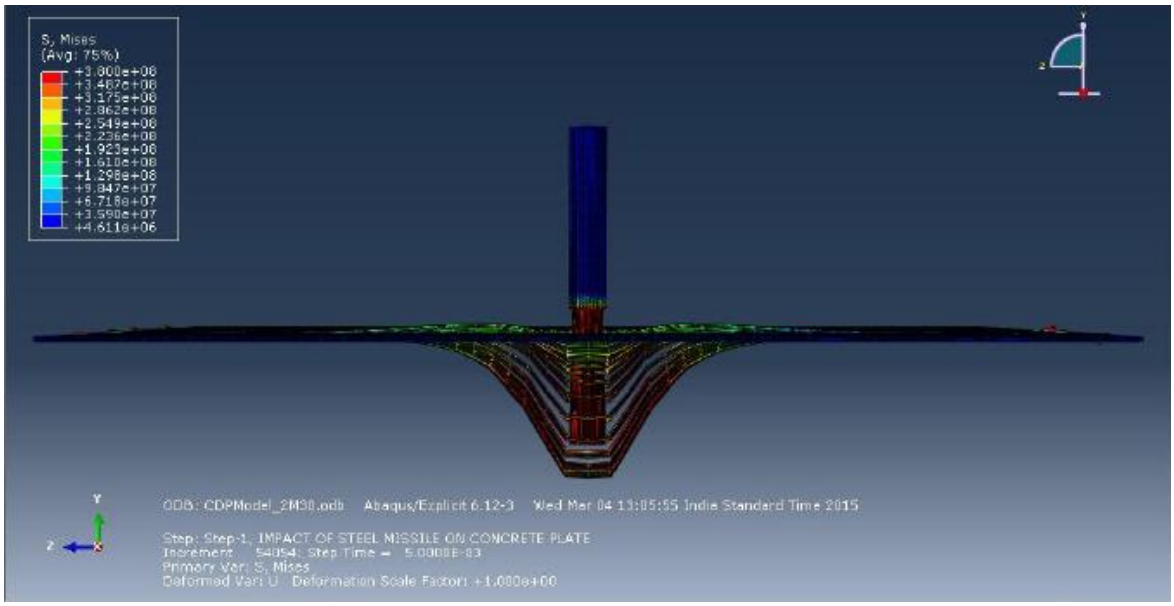

Figure 8. CDP model Case 2(b) – von Mises stress results for the rebars and the missile.

Consistent with the ABAQUS user's manual, the energy output is particularly important in checking the accuracy of the solution in an explicit dynamic analysis. In general, the total energy (ETOTAL) should be a constant or close to a constant; the "artificial" energies, such as the artificial strain energy (ALLAE), the damping dissipation (ALLVD), and the mass-scaling work (ALLMW), should be negligible compared to "real" energies, such as the strain energy (ALLSE) and the kinetic energy (ALLKE). A review of the ABAQUS results history file output indicates that the total energy for all four cases analyzed here is almost constant throughout the time interval of 5 ms. This check provides confidence in the numerical solution obtained using ABAQUS.

COMPARISON OF CASE RESULTS

Comparison of results from similar cases provides some meaningful insights related to the response of the barrier to missile impacts. The authors compare the missile impact response of the plain concrete barrier for Case 1(a) and Case 2(a), representing the BC model and the CDP model, respectively. Similarly, Case 1(b) and Case 2(b) are compared to illustrate differences in the predicted response of the reinforced concrete barrier.

Case 1(a) And Case 2(a) Comparison

The analysis of the plain concrete barrier using the BC model (Case 1 [a]) shows that under the effect of missile impact, degradation of material begins in the impact zone and in close vicinity of the contact area. This occurs when strains in the concrete elements exceed yield strain, or more precisely in ABAQUS terms, the cracking strain. However, all elements outside of the impact zone exhibit strains less than the cracking strain, indicating a punching shear failure. This behavior is consistent with the ABAQUS description of this model as a BC model. Degradation of concrete begins at 5 ms. On the other hand, the analysis using the CDP model (Case 2[a]) does not indicate any material degradation. However, in the CDP model, the plate deforms beyond the elastic limit in the impact zone and its vicinity. The leading end of the missile, which remains in contact with the concrete, sustains a state of yield at 5 ms.

Case 1(b) And Case 2(b) Comparison

The analysis of the reinforced concrete barrier using the BC model (Case 2[a]) also shows clear degradation of concrete, along with excessive deformation of a few steel rebars in the impact zone. The stress mapping indicates that the rebar elements accumulate tensile stresses beyond material yield. In the BC model, the entire steel missile sustains stresses beyond its yield strength. The concrete in the impact zone and at the supports in some places exceeds the failure strength within the impact duration of 5 ms.

The analysis using the CDP model (Case 2[b]) shows a similarly high state of stress only in the impact zone and its vicinity. The concrete and rebar exhibit stresses in excess of the material yield stresses in the impact zone. Similar to Case 1(b), the steel rebar exhibits significant deformation but of a different form than in the reinforced BC model. The analysis also indicates that the leading end of the steel missile sustains yield stresses.

EMPIRICAL METHODS TO DESIGN CONCRETE BARRIER

General design criterion 4 of Appendix A to 10 Code of Federal Regulations (CFR) 50 requires that structures, systems, and components important to safety be protected from the effects of missiles. Missile barriers and protective structures are designed to withstand and absorb missile impact loads to prevent damage to safety-related components. Empirical relationships, typically used to predict missile penetration, are based on the National Defense Research Committee (NDRC) modified formula for concrete and for steel.

Concrete (Modified NDRC Formula)

$$X = \left[4KNWd\left(\frac{V}{1000d}\right)^{1.8}\right]^{0.5} \text{ for } {}^{x}/_{d} < 2.0. \tag{1a}$$

$$X = KNWd\left(\frac{V}{1000d}\right)^{1.8} + d \text{ for } {}^{x}/_{d} > 2.0 \tag{1b}$$

where X is the penetration depth (inches); K is the experimentally obtained material coefficient $180\sqrt{f_c}$, where f_c is the concrete compressive strength in kips per square inch; N is the missile-shape factor (minimum value is 0.72); W is the missile weight in pounds (lb); d is the diameter of the missile (inches); and V is the missile velocity in feet per second (ft/sec).

Introducing the parameters for the analyzed cases in Equation (1a), x/d = 8/16 = 0.5, V = 150m/sec (492 ft/sec), d = 40 cm (16 inches), f_c = 50 N/mm^2 (7353 psi), ρ = 7850kg/m^3, $K = 180\sqrt{f_c} = 2.1$, $= {}^{\pi \cdot d^2}/_{4} \cdot \mathrm{L} \cdot \rho = 3.14 \cdot \frac{0.16m^2}{4} \cdot 0.5\mathrm{m} \cdot 7850 \cdot 2.28\, {}^{lbs}/_{m^3} = 1124\mathrm{lbs}$, the penetration depth (X) is calculated as 14.16 inches. The length (L) of the missile is taken as 0.5 m. Indeed, this exceeds the barrier thicknesses of 8 inches and 12 inches for the plain concrete and reinforced concrete barriers, respectively.

The scabbing thickness t_s and perforation thickness t_p are given by the following equations:

$$t_s = d \cdot \left[2.12 + 1.36 \cdot \left({}^{x}/_{d}\right)\right] \text{ for } 0.65 < {}^{x}/_{d} < 11.75 \tag{2a}$$

$$t_s = d \cdot \left[7.91 \cdot \left({}^{x}/_{d}\right) - 5.06 \cdot \left({}^{x}/_{d}\right)^2\right] \text{ for } {}^{x}/_{d} < 0.65 \tag{2b}$$

$$t_p = d \cdot \left[1.32 + 1.24 \cdot \left({}^{x}/_{d}\right)\right] \text{ for } 1.35 < {}^{x}/_{d} < 13.5 \tag{3a}$$

$$t_p = d \cdot \left[3.19 \cdot \left({}^{x}/_{d}\right) - 0.718 \cdot \left({}^{x}/_{d}\right)^2\right] \text{ for } {}^{x}/_{d} < 1.35 \quad (3b)$$

Based on the parameters of the cases analyzed, the value of x/d =14.16/16 =0.885, and therefore, using equations (2a) and (3b), the required minimum plate thickness to avoid perforation is calculated as follows:

$$t_p = 16 \cdot [3.19 \cdot 0.885 - 0.718 \cdot (0.885)^2] = 36.177\ inch$$

Similarly, the required minimum plate thickness to avoid scabbing is calculated as follows:

$$t_s = 16 \cdot [2.12 + 1.36 \cdot 0.885] = 34.93\ inch$$

A new equation to predict the critical impact energy required for penetration has been recently developed by Bux and Rahman (2011):

$${E_{cp}}/{f_c d^3} = a\left({}^{H}/_{d}\right)^3 + b\left({}^{H}/_{d}\right)^2 + c\left({}^{H}/_{d}\right) + d \quad (4)$$

where E_{cp} is the kinetic energy of missile impact required to result in perforation of the concrete target, f_c is the unconfined compressive strength of concrete, d is the (cylindrical) projectile shank diameter, and H is the total thickness of the concrete target. Using the barrier and missile parameters considered in the analysis, H = 10 inches and d =16 inches, the critical impact kinetic energy required for perforation of the concrete target is:

$${E_{cp}}/{f_c d^3} = 0.174\left({}^{H}/_{d}\right)^3 + 0.169\left({}^{H}/_{d}\right)^2 + 0.0577\left({}^{H}/_{d}\right) + 0.2969 \text{ for } 0.69 < {}^{H}/_{d} < 14.86$$

$$E_{cp} = 653396\ Nm$$

Rahman et al. (2010) further modify the NDRC formulae in terms of critical energies required to scab and perforate the concrete targets for flat-nose hard missile impact, as shown below.

The critical impact energy for scabbing in SI units is as follows:

$${E_{cp}}/{f_c d^3} = \left(\frac{V_0}{d}\right)^{0.2} f_c^{-0.5} \left[52.84 - \sqrt{2789.4 - 903.9\left(\frac{H}{d}\right)}\right]^2 \text{ for } {}^{H}/_{d} \le 3.0 \quad (5a)$$

$${E_{cp}}/{f_c d^3} = \left(\frac{V_0}{d}\right)^{0.2} f_c^{-0.5} \left[51.35\left(\frac{H}{d}\right) - 105.34\right]^2 \text{ for } 3.0 < {}^{H}/_{d} \le 4.84 \quad (5b)$$

$${E_{cp}}/{f_c d^3} = \left(\frac{V_0}{d}\right)^{0.2} f_c^{-0.5} \left[1.389 \cdot 10^4\left(\frac{H}{d}\right) - 4.677 \cdot 10^4\right] \text{ for } 4.84 < {}^{H}/_{d} \le 18.0 \quad (5c)$$

and the critical impact energy for perforation is as follows:

$${E_{cp}}/{f_c d^3} = \left(\frac{V_0}{d}\right)^{0.2} f_c^{-0.5} \left[150 - \sqrt{22.53 \cdot 10^3 - 6.36 \cdot 10^3\left(\frac{H}{d}\right)}\right]^2 \text{ for } {}^{H}/_{d} \le 3.0 \quad (6a)$$

$$E_{cp}/f_c d^3 = \left(\frac{V_0}{d}\right)^{0.2} f_c^{-0.5}\left[54.46\left(\frac{H}{d}\right) - 71.96\right]^2 \text{ for } 3.0 < H/d \leq 3.8 \quad (6b)$$

$$E_{cp}/f_c d^3 = \left(\frac{V_0}{d}\right)^{0.2} f_c^{-0.5}\left[1.473 \cdot 10^4\left(\frac{H}{d}\right) - 3.774 \cdot 10^4\right] \text{ for } 3.8 < H/d \leq 18.0 \quad (6c)$$

Using the analysis case parameters, H (thickness of concrete plug) = 300 mm, V_o = 150 m/sec, and d (diameter of the projectile) = 0.4 m, the critical energy required for perforation is calculated to be E_{cp}= 452736 Nm. The total energy calculated using ABAQUS (5.53e+06 Joules) significantly exceeds the E_{cp} value predicted by Equation (4) and the equations given by Rahman et al. (2010).

The above evaluation illustrates the consistency of the stress and deformation response and the calculated total strain energies from the ABAQUS analysis and the penetration and perforation predicted from empirical relationships.

CONCLUSIONS

One of the objectives of the four case studies conducted to analyze the effects of the missile impact is to explore the contribution of reinforcement to barrier performance. This objective is actually an outcome of the primary purpose of the investigation regarding the physics of material behavior leading to geometric nonlinearities, the evolution and projection of failure in concrete, and the failure of the reinforcement in the impact zone.

The analysis results show that reinforcement alone cannot arrest perforation until a minimum concrete thickness is also provided. Another insight is that rebar placed in the facing layer is not very effective in controlling perforation. Rather, in the opinion of the authors, placing the reinforcement near the trailing face, which does not experience direct impact, improves barrier performance. In principle, this is because more of the trailing-face rebar is engaged in resisting the imparted energy to the barrier. The analyzed cases 1(b) and 2(b) predict significant rebar yielding and deformations, even though these cases assume the rebar is located at mid-depth. Indeed, standard code practice requires placement of minimum-shrinkage and temperature reinforcement in proximity to both the near and far faces. The current work is planned to be extended to better quantify the effectiveness of the rebar in barrier performance and to develop multilayer barrier designs so that concrete thickness can be significantly improved.

REFERENCES

Bureau of Indian Standards – 456-2000, Plain & Reinforced Concrete (2007).

Bux, Q., alias Latif, I., and Rahman, I.A. (2011), "Development of Empirical Formula Prediction on Critical Impact Energy for Perforation Phenomena on Concrete Structures," *Journal of Mathematics Research*, Vol. 3, No. 1, pp. 83-87.

Hsu, L.S. and Hsu, C-T.T. (1994), "Complete Stress-Strain Behaviour of High-Strength Concrete Under Compression," *Magazine of Concrete Research*, Vol. 46, No. 169, pp. 301-312.

Mokhatar, S. N. and Abdullah, R. (2012), "Computational Analysis of Reinforced Slabs Subjected to Impact Loads," University Tun Hussein Onn Malaysia, *International Journal of Integrated Engineering*, Vol. 4, No. 2, pp. 70-76.

Rahman, I.A.; Zaidi, A.M.A.; Bux, Q., alias Latif, I. (2010), "Review on Empirical Studies of Local Impact Effects of Hard Missile on Concrete Structures," *International Journal of Sustainable Construction Engineering & Technology*, Vol. 1, No. 1, pp. 71-95.